Direct and Inverse Modeling in EMG

Maghoul P[*], Mathieu P.A[**], Corinthios M[*],
[*]Dépt. génie électrique, École Polytechnique de Montréal,
[**]Institut de génie biomédical, Université de Montréal

Abstract—Muscle activity is accompanied by an electrical signal (electromyogram or EMG) which travels through a complex volume conductor before reaching the surface of the body. Most usually, this signal is recorded with surface electrodes since it is not invasive but due to its alterations induced by the volume conductor, information on the signal origin is difficult to obtain. In such a context, the use of a direct and inverse model could offer useful information to help analyze and take benefits of surface EMG signals. We are developing such a model in the context of improving the control of myoelectric prostheses capable of producing various movements This could be possible by exploiting the presence of anatomical compartments within large muscles such as the biceps and triceps brachii. If activation of those compartments could be individually activated, they could be used to activate modern myoelectric prostheses. To develop the models, a tank circled with recording electrodes and dipoles positioned at known positions was used. Preliminary results are presented here.

***Index Terms*—Electromyography, direct and inverse model, Poisson equation, myoelectric prosthesis.**

I. INTRODUCTION

In recent years, a lot of research has been done to improve the quality of life of upper arm amputee persons. Most available prostheses are electrically powered and controlled through surface EMG signals. With amputations around and above the elbow, the number of usable muscles to control a prosthesis is restricted. With intramuscular electrodes more recording sites could be obtained but for long term use, this approach is not practical due to possible electrode displacements induced by the repetitive contractions of the muscle and the risks of infection where the skin is pierced. In order to increase the number of surface control sites, the presence of up to 6 anatomic compartments innervated by individual nerve branches within the biceps brachial [1] is being investigated in our group. To help associate the EMG potential distribution collected over the biceps to those compartments, an inverse EMG model would be very useful. In the field of EMG, the one can find the models of analytic method and of numeric method [2,3]. In our case in this step, we choose the analytic approach.

II. METHODOLOGY

A. Experimental Methods

As a simple model of the arm, a tank surrounded by 16 equidistant electrodes and filled with saline solution was used. Up to three dipoles were placed at various locations in the tank (Fig.1A).

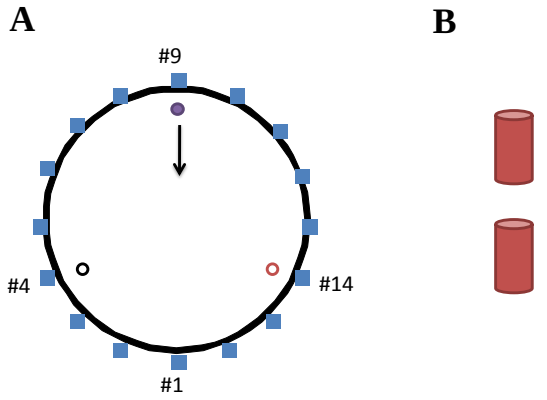

Fig.1. **A:** schematic of the tank (175 mm of diameter) circled by 16 equidistant Ag/AgCl electrodes of 10 mm in diameter and filled with a saline solution In this figure, the position of two dipoles is fixed (near electrodes #4 and #14) while the third one was moved radially step by step toward the center of the tank. **B:** each dipole is made of two cylindrical sintered Ag/AgCl of 1.5 x 3 mm separated by 2 mm and placed perpendicular to the bottom of the tank and few mm above the plane of the recording electrodes.

The dipoles (Fig.1B) were activated with sinusoidal currents of 22 to 45 Hz. Initially, one dipole was placed at the periphery of the tank and moved radially toward its center. Then, two

dipoles were used: one located near one electrode while the other was moved from the border to the center of the tank. Finally, three dipoles were used: two of them had the fixed position next to the border of the tank (open circles in Fig.1A) while the third one was moved from the border up to the center of the tank. The collected signals were analyzed off-line. The root mean square (RMS) values is obtained at each electrode recording from each dipole frequency contribution was used.

For the positioning of the dipoles, the power spectrum of the signal at one electrode was used to determine how many dipoles were present in the tank. Then, for comparison with the simulation results, the RMS value of the signal of each of those dipoles was obtained before their addition. To locate those dipoles the inverse model was used.

B. Direct Problem

For the direct and inverse model, we used the Poisson equation (1):

$$\nabla^2 V(r) = -j(r)/\sigma \quad (1)$$

$$\frac{\partial V}{\partial n} = 0 \quad (2)$$

where $V(r)$is the electric potential associated with the current density source $j(r)$ within an homogenous medium of conductivity σ while (2) is associated to the limited dimensions of the tank. To simulate the experimental potential distribution recorded around the tank by our dipoles, we will have image phenomenon because of finite dimension of the tank (Fig. 2).

To obtain the potential through the tank, we extensively used the work of Lambin and Troquet [4] and Okada [5] to produce our models. To simulate the potentials around the tank, we have to solve:

$$V(r) = (p.\nabla)G(r,r') \quad (3)$$

where p is the dipole moment. Furthermore $G(r,r')$ is green function and Φ_N is normalized solution of the Strum-Liouville problem defined by the eigenvalues of (4):

$$\nabla^2 \Phi_N + \lambda_N \Phi_N = 0 \quad (4)$$

The Green function was used to solve (1):

$$G(r,r') = \sum_{n\neq 0} \Phi_N \Phi_N^* / \lambda_N \quad (5)$$

where r is the coordinates of the observation point and r' those of a dipole. Due to the image phenomenon reflections at the bottom of the tank and at the top of the liquid give rise to two sets of dipole images located at r_j' and r_k'' that r_k'' is the location of dipole image relative to the bottom of the tank, z_0''. Furthermore the dipole image relative to the top of the liquid in tank, z_1''. r_j' is the image of z_0'' relative to the top of the tank, z_1'. Finally by solving (3) with conditions (4) and (5), equation (6) is reached.

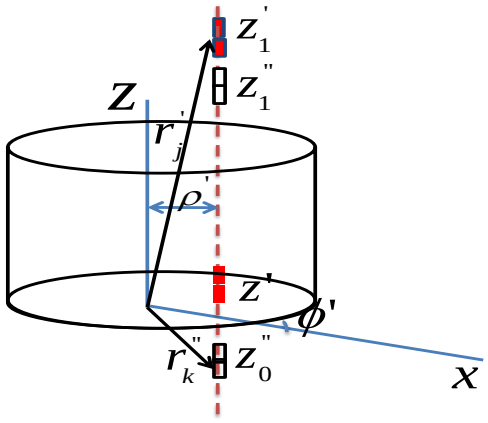

Fig. 2. The image phenomenon from the front section where the dipole is positioned at $z'(\rho'\varphi'z')$. Illustration modified from Lambin and Troquet [4].

$$V_z(\rho\phi z) = \frac{-p_z}{L^2\sigma}\sum_{m=0}^{\infty}(2-\delta_{m0}) \times cos[m(\phi-\phi')]\sum_{n=1}^{\infty} nI_m\left(\frac{n\pi\rho'}{L}\right)\left[K_m\left(\frac{n\pi R}{L}\right) - \frac{K_m'\left(\frac{n\pi R}{L}\right)}{I_m'\left(\frac{n\pi R}{L}\right)} I_m\left(\frac{n\pi R}{L}\right)\right] cos\left(\frac{n\pi z}{L}\right) sin\left(\frac{n\pi z'}{L}\right) \quad (6)$$

where I_m, K_m is the first and second kind of modified Bessel and δ is delta function.

C. Electrode size

Our electrodes being not punctual, a convolution equation taking care of the electrodes area was used to simulate their potentials. A simple equation assuming a constant value, equal to the inverse of the electrode area was used:

$$h_{size} = \frac{1}{S} \quad (10)$$

where S is the electrode area. In case of a circular electrode with radius r, its transfer function will be:

$$H_{size} = \frac{J_1(2\pi r f_z)}{\pi r f_z} \quad (11)$$

where $J_1(k)$ is the first-order Bessel function of the first kind and f_z is the spatial frequency which is defined by (12).

$$\lambda = \frac{1}{f_s} \quad (12)$$

D. Inverse Problem

For the inverse model, the gradient method was used to minimize a cost function (13) evaluating the differences between values obtained with the Poisson equation and the experimental results:

$$C = \sum_{i=1}^{N} (V_{i,calculated} - V_{i,observed}) \quad (13)$$

Due to the small size of our dipole (1.5 x 3 mm cylinder), they only affect the three closest electrodes. With the inverse model, potentials at those electrodes were used to identify where the moving dipole was positioned in the tank. A circle with a radius proportional to the voltage associated with that dipole at each of those electrodes was traced with the electrode positions as centers. The common intersection point of those circles gives the assumed position of the mobile dipole.

III. Results

The results with two dipoles (one in a fixed position near an electrode and one moving radially from the border to the center of the tank) are presented in Fig.3A for the three electrodes where a signal could be recorded. As the mobile dipole is getting farther from the recording sites, the signals decrease exponentially but does not reach zero due to the fixed dipole. That value was subtracted and the obtained signal was evaluated by (10) where ρ' parameter of (6) was used to estimate the position the mobile dipole in the tank as illustrated in Fig.3B. In presence of three dipoles (two fixed and one mobile), (Fig.4A), the voltages recorded at the three involved electrodes are varying as with two dipoles. With the inverse model, location of the mobile dipole was more precise up to 40 mm from the border of the tank than further away (Fig. 4.B). It should be attention, the value which is showed in Fig.3 and Fig.4 are the RMS value of signals in related electrodes. RMS value is not a linear function so to obtain this value, the effect of each dipole in time should be added and then its RMS value is calculated. As it can be seen in Fig.4A, the RMS values of potential at electrodes 4 and 14 are constant. The reason that can

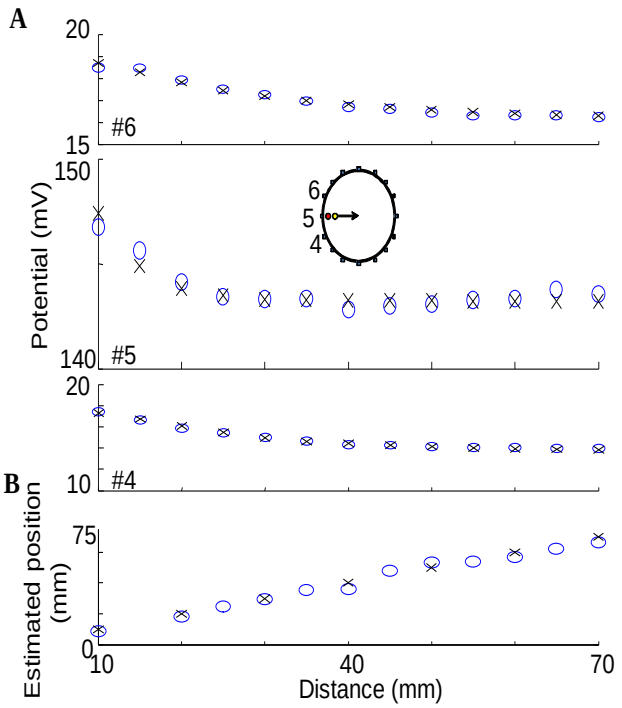

Fig.3 A: potentials recorded at three electrodes as a dipole is moved radially from the border to the center of the tank while a second one is kept fixed near the border. Experimental data (circles) and simulation results (crosses). B: real (circles) vs estimated distance (crosses) of the mobile dipole.

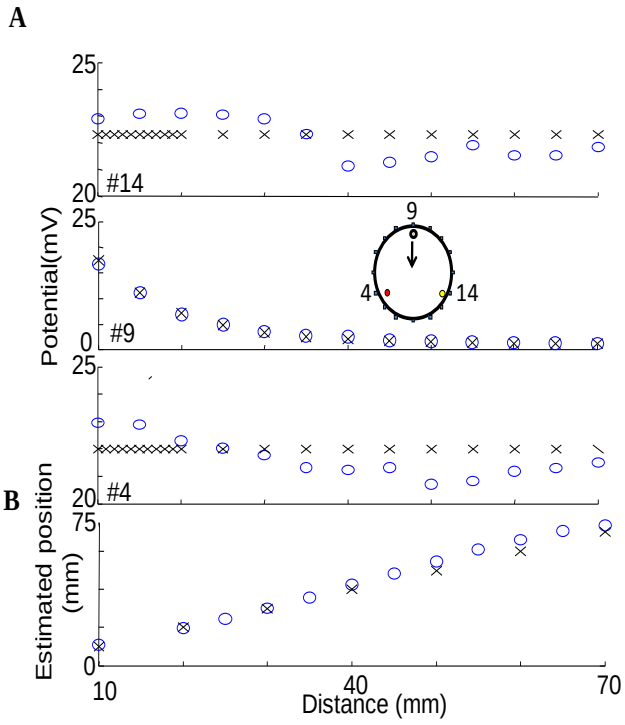

Fig.4. A: experimental data (circles) and simulation results (crosses) with two fixed dipoles (near electrodes #4 and #14) and a third one moving radially toward the center of the tank. B: estimated (crosses) vs real distance position (circles) of the mobile dipole.

describe this phenomenon is that the dipoles are far away from each other so they cannot affect to each other considerably as the constant RMS value has been seen. In other words, the electrodes which their signals recorded, affect only by one dipole not like previous test.

There exist a lot of factors that are caused in the experiment like as the time when the data do not stay in constant values. For example the environment noise that may come from the power line. Another error source can be the dipole position deviation that may exist along the z-axis in the test. These factors make the varying in signals through electrodes 4 and 14.

IV. Discussion

With a dipole placed near the border of the tank and a second one moved toward the center, the direct model was in error close to the border (Fig. 3). This could be due to the lack of perpendicularity of the tube holding the dipoles (eqn. 6 is developed for a dipole perfectly aligned with the Z-axis). As expected, this effect has more effect when the mobile dipole is near the border of the tank than closer to the center. With the inverse model, the larger error is found when the mobile dipole is approaching the center of the tank (Figs. 3B and 4B). This is associated to the exponentially diminishing contribution of the dipole to the potentials recorded around the tank which makes the detection of its position more difficult.

In the future, inhomogeneities will be insert in the tank to simulate some of the conductive medium (bone, fat, blood vessels) The presence of many boundaries conditions will make the analytical solution too difficult to manage with an analytical approach. A numerical solution, like the Finite-Difference Time-Domain Method (FDT) will then have to be considered.

Acknowledgment

Thanks to David Filion for the experimental data collection. Research supported by NSERC grant #156144-2010.

References

[1] Segal, L., "Neuromuscular compartments in the human biceps brachii muscle",Neuroscience Letters, Volume 140, Issue 1, 8 June 1992, Pages 98-102

[2] Lowery, M. M., N. S. Stoykov, A. Taflove, and Kuiken, "A multiple-layer finite-element model of the surface EMG signal," *IEEE Trans BME* **49**, 446–454 (2002).

[3] Gootzen, T. H., D. F. Stegeman, and A. Van Oosterom, "Finite limb dimensions and finite muscle length in a model for the generation of electromyographic signals," *Electroenc Clin Neurophysiol,* **81**, 152–162 (1991).

[4] P. Lambin, and J. Troquet, "Complete Calculation of the Electric Potential Produced b a Pair of Current Source and Sink Energizing a Circular Finite-Length Cylinder", *J. Appl. Phys*, 54:7, 4174-4184, 1983.

[5] R.H Okada, "Potentials Produced by an Eccentric Current Dipole in a Finite-Length Circular Conducting Cylinder", *IRE*. *Trans. Med. Electron*, 7, 14-19, 1956.

[6] D.K Cheng, *Field and Wave Electromagnetics.* Addison-Wesley Publishing Co., 1983.

[7] T.H.J.M Gootzen, and D.F Stegeman, and A, Heringa, "On Numerical Problems in Analytical Calculations of Extracellular Fields in Bounded Cylindrical Volume Conductors", *J. Appl. Phys*, 66:9, 4504-4508, 1989.

[8] J.K Jackson , *Classical Electrodynamics.* Wiley, New York, 1962.

[9] J. Malmivuo, and R. Plonsey, *Bioelectromagnetism.* Oxford U. Press, 1995.

[10] M.O Sadiku, *Numerical Techniques in Electromagnetics,* CRC Press, 2009.

[11] K. Saitou, and T. Masuda, Okada M. **"**Depth and intensity of equivalent current dipoles estimated through an inverse analysis of surface electromyograms using the image method", *BMES* 1999, Vol. 37, pp 720-726.

[12] S.A Schelkunoff, *Electromagnetic Waves* (Van Nostrand Co., New York, 1943)

[13] Fuglevand, A., D. Winter, A. Patla, and D. Stashuk, "Detection of motor unit action potentials with surface electrodes: influence of electrode size and spacing," Biol cybern 67, 143–153, 1992.